

Interlayer tunnelling spectroscopy of charge density waves

Yu I Latyshev¹, P Monceau², A P Orlov¹, S A Brazovskii³ and Th Fournier²

¹ IREE RAS, Mokhovaya 11-7, 125009 Moscow, Russia

² CRTBT-CNRS, BP 166, 38042 Grenoble, France

³ LPTM-CNRS, Université Paris-Sud, 91405 Paris, France

Received 2 October 2006

Published 4 December 2006

Online at stacks.iop.org/SUST/20/S87

Abstract

A brief review of recent results on interlayer tunnelling spectroscopy of layered charge density wave (CDW) materials is presented, demonstrating the high capability of this method for studies of this electron condensed state. We discuss some features observed in comparison with high temperature superconductors (HTS).

(Some figures in this article are in colour only in the electronic version)

1. Introduction to interlayer tunnelling in HTS materials

The method of interlayer tunnelling is based on the layered crystalline structure of some highly anisotropic materials where elementary, atomically thin conducting layers are separated by elementary isolating layers (figure 1(a)). The transport along the layers in these materials is provided by metallic intralayer conductivity while the transport across the layers occurs via interlayer tunnelling. In a case when the layered structure of that type undergoes, at low temperatures, a phase transition into an electron condensed state (e.g. superconducting or CDW state) the interlayer tunnelling may be used as an effective tool to study that state [1].

In many cases as in layered superconductors the amplitude of the order parameter (OP) becomes vertically modulated, while phases in neighbouring layers remain coupled. That yields effects of both types in interlayer tunnelling, one related to phase interference (DC intrinsic Josephson effect) or phase decoupling (appearance of Josephson vortices in parallel magnetic field). Another type, as quasiparticle tunnelling over a superconducting gap, is related to the amplitude of the OP. Many fundamental properties of high temperature superconductors related to the symmetry of the OP [2], gap/pseudogap spectroscopy [3] and dynamics of Josephson vortex lattices [4] have been explored using the interlayer tunnelling technique. One of the attractive features of the method when compared with some other widely used spectroscopic techniques such as IRS, ARPES and STM is the possibility to get information from the bulk of the material.

Figure 1(b) illustrates the DC intrinsic Josephson effect on the micron sized mesa structure of layered HTS superconductor Bi-2212. The Fraunhofer pattern observed on this device shows that the scale of periodicity on the external magnetic field is higher than that observed on conventional Josephson junctions of the same lateral size by three orders of magnitude. This is a direct demonstration of the atomic scale smallness of the elementary junction size along the *c* axis.

For stacks of bigger sizes $L > \lambda_J$ (where λ_J is the Josephson penetration depth $= s\lambda_c/\lambda_{ab}$ with $\lambda_{c,ab}$ the anisotropic London penetration depth) a parallel magnetic field above some threshold value H_{c1} decouples phases between neighbouring junctions by creation of Josephson vortices (JVs) [7]. A JV represents a phase topological defect. The circulation around its nonlinear core gives a phase variation of 2π . At higher fields the inter-vortex interaction leads to their ordering into the Josephson vortex lattice (JVL) [8]. The JVL motion induced by a current applied across the layers is accompanied by Josephson emission and may be identified by the Shapiro step response to the external microwave field. Experiments of that type [9] revealed the existence and the high coherence of the driven JVL.

2. Interlayer tunnelling in the CDW state

Recently, the method of interlayer tunnelling has been extended to other types of layered materials like layered manganites [10] and layered CDW materials [11]. The CDW condensed state is, in many respects, similar to the superconducting state. Below the Peierls transition temperature an energy gap in electronic spectra is opened at

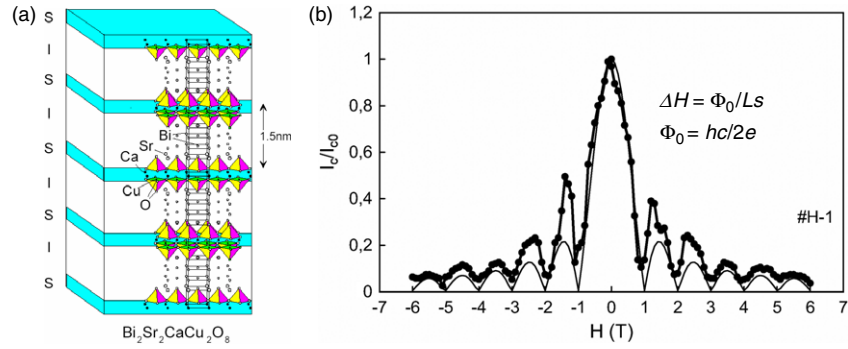


Figure 1. (a) Schematic view of microscopic layer structure of layered superconductor $\text{Bi}_2\text{Sr}_2\text{CaCu}_2\text{O}_{x+8}$ where elementary superconducting layers S are separated by elementary insulating (I) layers with spacing $s = 1.5 \text{ nm}$. (b) Fraunhofer pattern of the critical Josephson current across the layers as a function of magnetic field parallel to the layers H [5] on Bi-2212 mesa with lateral size of $1.4 \mu\text{m}$. The solid line is the theoretically predicted dependence [6] $I_c/I_{c0} = (\sin x)/x$ with $x = \pi s L H / \Phi_0$, where L is the lateral size of the mesa perpendicular to the field.

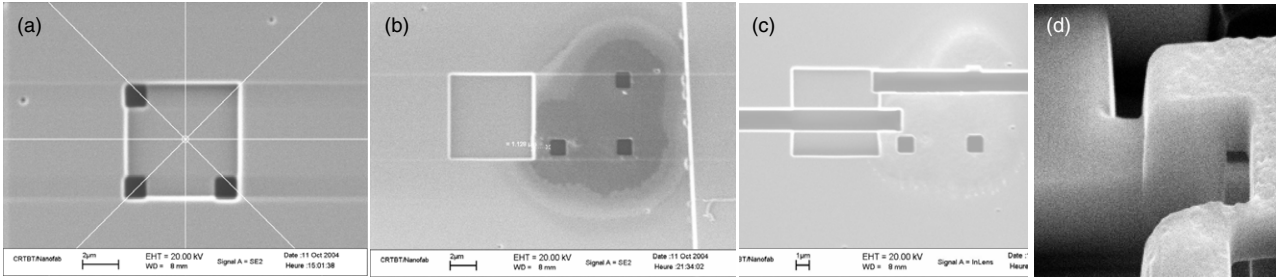


Figure 2. ((a)–(c)) Stages of the double sided FIB processing technique for fabrication of the stacked structure; (d) SEM image of the structure. The structure sizes are $1 \mu\text{m} \times 1 \mu\text{m} \times 0.3 \mu\text{m}$.

the Fermi surface as well. The difference is as follows. The superconducting state is formed by the coupling of electrons on the opposite sites of the Fermi surface. The total momentum of this pair (Cooper pair) is equal to zero. In contrast, in the CDW condensed state the coupling occurs between electrons and holes at the opposite parts of the Fermi surface. Because of the negative effective mass of a hole, the pair of that type has a total momentum $2p_F$ or a wavevector $2k_F$. As a result the density of condensed carriers is spatially modulated forming a charge density wave [12]. In the case when the CDW is incommensurate with the underlying lattice its order parameter can be expressed as $\Delta_0 = A \cos(Qx + \varphi)$ with $Q = 2k_F$ the CDW wavevector and φ an arbitrary phase. A Peierls transition is preferable for compounds possessing considerably flat parts of the Fermi surface separated by $2p_F$ (nesting condition). That is typical for low-dimensional (quasi-1D or quasi-2D) crystals containing conducting elementary chains or conducting planes.

For a number of typical CDW materials of MX_3 type (M—transition metal, X—chalcogen) the conducting chains are assembled in elementary conducting layers isolated from each other by a double barrier of insulating prism bases [11]. For NbSe_3 that results in a very high interlayer conductivity anisotropy $\sigma_a^*/\sigma_b \sim 10^{-3}$ at low temperatures compared with the intralayer anisotropy $\sigma_c/\sigma_b \sim 10^{-1}$. In the Peierls state, similar to layered superconductors, the amplitude of the OP is modulated across the layers while phases remain coupled. That provides a ground studying for CDW gap spectroscopy by interlayer tunnelling.

The CDW gaps and the zero bias conductance peak (ZBCP) have been identified in NbSe_3 using this method [11, 13]. Here we present a short review of our recent studies on interlayer tunnelling spectroscopy including observation and studies of new collective states with their energy lying inside the CDW gap.

3. Stacked structure fabrication and characterization

The stacked structures used for interlayer tunnelling spectroscopy in HTS materials usually have micron scale lateral sizes and contain several tens of elementary junctions. The small size of the stacks provides phase coherence of interlayer tunnelling [14] and highly reduced self-heating effects [15]. Recently the focused ion beam (FIB) technique has been developed for fabrication of those structures [16]. We applied this technique on CDW materials NbSe_3 and o-TaS_3 .

The stages of fabrication are shown in figures 2(a)–(c). At the first stage (figure 2(a)) a square trench of typical size $6 \mu\text{m} \times 6 \mu\text{m}$ is etched on one side of a thin single crystal by FIB to the depth of $d/2 + \delta$ where d is the thickness of the crystal and δ is the small excess depth. Typically, for $d = 1 \mu\text{m}$ we selected $\delta = (0.05–0.1)d$. The depth of etching is calculated from the time of etching the same area under the same etching conditions through the whole thickness of the crystal. The position of the trench is marked by small spots at the corners etched through the rest of the crystal thickness. At the second stage (figure 2(b)) the crystal is turned over and

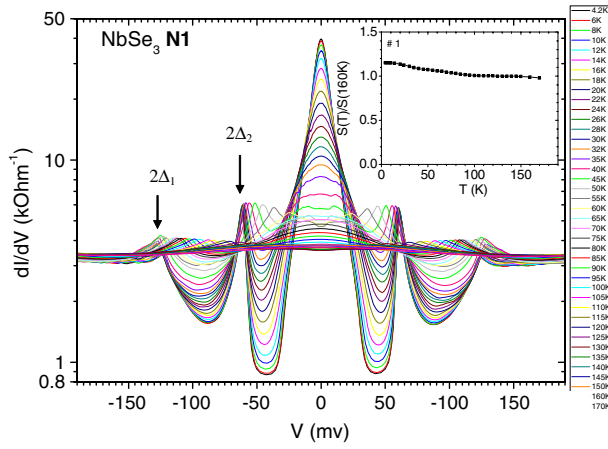


Figure 3. Temperature evolution of interlayer tunnelling spectra of NbSe_3 within the temperature interval 170–4.2 K; the inset shows temperature dependence of the integral $S = \int_{-V_0}^{V_0} dI/dV(V) dV$.

a second trench is etched on the opposite side of the crystal near the first one to the same depth. The stacked junction with thickness of 2δ is thus formed between the trenches. At the third stage (figure 2(c)) the stacked structure is trimmed to the whole width of the crystal. The typical junction is shown in figure 2(d).

4. CDW gaps and zero bias conductance peak

The interlayer tunnelling spectra have been measured by four probes. The greatest part of the applied voltage is dropped at the stacked junction due to the very high anisotropy conductivity along and across the conducting planes. The I – V characteristics of the junction have been measured using a programmable current source and a nanovoltmeter. The tunnelling spectra $dI/dV(V)$ have been obtained by numerical differentiation of the I – V data.

The evolution of the interlayer tunnelling spectrum for NbSe_3 with decreasing temperature is shown in figure 3. NbSe_3 undergoes two Peierls transitions at $T_{p1} = 145$ K and at $T_{p2} = 59$ K.

The appropriate CDW gaps appear as peaks in the spectra at $V_{g2} = 2\Delta_2$ and $V_{g1} = 2\Delta_1$ below the Peierls transitions. At low temperatures $V_{g2} = 50$ – 60 mV and $V_{g1} = 130$ – 150 mV. Along with the gap peaks a strong zero bias conductance peak (ZBCP) appears at low temperatures. The gap values found are consistent with STM [17], optics [18] and low temperature ARPES data [19] as well as with point contact spectra NbSe_3 – NbSe_3 along the a^* axis [11]. The results show that only one elementary tunnel junction in the stack is working at high bias voltage; we consider this single junction as the weakest elementary junction, where the CDW phase decoupling occurs with the increase of V . We interpreted the ZBCP anomaly as the result of coherent interlayer tunnelling of non-condensed carriers localized in small pockets on the Fermi surface [13]. Both the height and the width of ZBCP characterize the stack quality. For the best samples, the ratio of the ZBCP height to the background value at $V > 2\Delta$ reaches 30 while the ZBCP half-width is 10 mV.

We found that, in spite of very sharp changes of $dI/dV(V)$ below the Peierls transitions, the total spectral weight S is nearly unchanged below and above transition temperatures (inset of figure 3). We defined S as the integral of dI/dV curves between the fixed voltages from $-V_0$ to $+V_0$, with V_0 being considerably above the highest CDW gap. That result indicates that opening of the CDW gaps nearly does not affect the total number of single-particle states. The small variation observed may be related to the weak dependence of the interlayer barrier transparency with temperature. A similar behaviour has been recently demonstrated for interlayer tunnelling in HTS materials [20]: the opening of the pseudogap and superconducting gaps does not affect the integral density of states.

5. Interaction of two CDWs in NbSe_3

The very sharp gap peaks observed allowed us to measure very precisely temperature variation of the gap value. As was noticed earlier [11] and in more precise recent measurements [21] both gaps follow the BCS type dependence quite well.

Below T_{p2} two CDWs coexist in NbSe_3 . The question whether they are independent or interacting with each other has been widely debated in the literature. The first observations evidenced that the formation of the CDW2 has a negligibly small effect on the first one. That was based on the facts that no observable change occurs below T_{p2} in either the position [22] or intensity [23] of the diffraction spots associated with the first CDW. However, another experimental fact pointed out the possible phase locking effect between the two CDWs. Namely, the wavevectors characterizing the two CDWs [23, 24] $q_1 = (0, 0.243, 0.5)$ and $q_2 = (0.5, 0.263, 0.5)$ in units of the reciprocal unit lengths satisfy the approximate relation

$$2(q_1 + q_2) \cong (1, 1, 1) \quad (1)$$

i.e. twice their sum is a reciprocal lattice vector. Some authors [25, 26] considered that as the evidence of phase coupling between the two CDWs below T_{p2} . The analysis based on the simple Ginzburg–Landau theory [26] pointed out that a phase-locking effect can be accompanied by the small enhancement of CDW1 energy gap below T_{p2} . That follows from the additional term in the Ginzburg–Landau free energy related to the joint commensurability effect [26]:

$$F_2 = F_1(\Delta_1) + A_2\Delta_2^2 + B_2\Delta_2^4 + B_+\Delta_1^2\Delta_2^2 \cos 2(\varphi_1 + \varphi_2) \quad (2)$$

where $F_{1,2}$ are free energies below $T_{p1,p2}$ and $\varphi_{1,2}$ are corresponding phases of the order parameters $\Delta_{1,2}$.

Recent studies revealed some features of the interaction between the two CDWs in the dynamical state, when one or both CDWs are in a sliding state. In particular, it was found that the threshold for CDW1 depinning decreases below T_{p2} [27]. Also it was found that the sliding of both CDWs below T_{p2} causes a correlated and opposite shift of the satellite spot positions, keeping the projection of $q_1 + q_2$ along the chain unchanged [28]. That was interpreted as a dynamical decoupling of CDWs.

However, the static phase-locking effect and the corresponding enhancement of the CDW1 gap below T_{p2} still

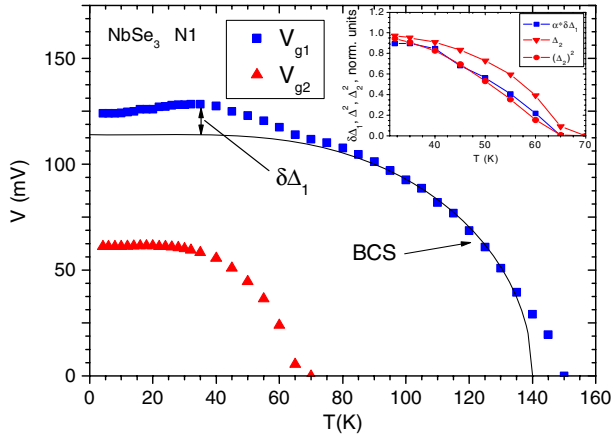


Figure 4. Temperature dependences of the lower $2\Delta_2$ and the upper $2\Delta_1$ CDW gap values in NbSe_3 . The solid line is a fit to the BCS type dependence in the temperature interval 70–140 K. The inset shows a comparison of temperature dependence of the enhancement of Δ_1 , $\delta\Delta_1(T)$ with dependences $\Delta_2(T)$ and $\Delta_2^2(T)$.

has not been experimentally verified. That was partly related to the absence of a reliable and sensitive technique for CDW gap spectroscopy.

Using an interlayer tunnelling technique we succeeded in revealing this interaction.

As follows from figure 4, the opening of the CDW gap Δ_2 below T_{p2} , indeed, leads to the enhancement of the gap Δ_1 , $\delta\Delta_1$. The effect is shown to be of the second order in Δ_2 (inset in figure 4) and is relatively small, the maximum enhancement of $\delta\Delta_1/\Delta_1$ being ≈ 0.1 .

6. Intragap CDW states

As was mentioned above the incommensurate CDW (ICDW) is characterized by the OP $\Delta_0 = A \cos(Qx + \varphi)$. The uniform ground state in the ICDW state with $A(x) = \text{const}$ is degenerated with respect to the phase shift by π that changes A by $-A$. That leads to the possibility of non-uniform ground state that can be realized by local change of the phase by π and simultaneous acceptance of one electron from the free band to conserve electro-neutrality. The resulting state with $A = \tanh(x/\xi_0)$ is known as the amplitude soliton (AS) [28]. The AS has an energy $E_s = 2\Delta/\pi$ that is lower by $\sim \Delta/3$ than the lowest energy of an electron in a free band Δ . Therefore, free electrons near the band edge tend to be self-localized into AS states. Experimentally the existence of AS states has been reliably demonstrated only for dimeric compounds like polyacetylene. Using an interlayer tunnelling technique we undertook an attempt to find the AS states in inorganic MX_3 compounds with commensurability parameter m close to $m = 4$. To avoid the masking effect of the ZBCP we used a high temperature regime where the ZBCP is suppressed, or a low temperature regime in the presence of the high magnetic field parallel to the layers that narrows the ZBCP [11]. In both cases, in addition to a peak at $V = 2\Delta$, we found an additional peak at $V = 2\Delta/3$ (figures 5(b), (c)) which was interpreted as the result of interlayer tunnelling with a transition of pocket carriers to the AS levels [29].

Table 1. Duality of phase topological defects in layered HTS and CDW systems.

HTS	CDW
Flux	Charge
$\Phi_0 = hc/2e$	$Q_0 = 2e$
$H \parallel \text{layers}$	$E \perp \text{layers}$
H_{c1}	E_t

The interlayer tunnelling studies of another CDW compound, $o\text{-TaS}_3$, also demonstrated the existence of the ASs in that compound in the ICDW state. $o\text{-TaS}_3$ experiences a transition to the commensurate CDW (CCDW) state at 130 K. At the CCDW state the phase of the OP is locked by the lattice periodicity and the AS states with an acceptance of one electron are forbidden. As a result, we found an increase of the observed tunnelling gap by $1/3$ followed by a transition from the ICCDW to the CCDW state [30].

7. Phase decoupling effects on interlayer tunnelling in layered CDW materials

Another remarkable feature that appears at lower energies within the CDW gap is a sharp voltage threshold V_t for onset of the interlayer tunnelling conductivity (figures 5(b), 6(a) and 7(a)). The value of V_t at low temperatures was found to be close to the energy of 3D CDW ordering kT_p (T_p is the Peierls transition temperature) for both CDWs in NbSe_3 and for $o\text{-TaS}_3$ (figure 6(b)). Therefore, V_t was attributed to the energy of the CDW phase decoupling between the neighbouring layers.

Brazovskii developed a model that describes phase decoupling via the subsequent formation in the weakest junction of an array of dislocation lines (DLs) [31], the CDW phase topological defects. The DLs are oriented across the chains. They appear as a result of the shear stress of the CDW induced by the electric field. As in a case of Josephson vortices the circulation around the DL core gives a phase variation of 2π . That corresponds to the CDW elementary charge $2e$ per chain. The excess charge of the DL accumulates the electric field within the DL core. In the vertical direction the DL core has atomic size, i.e. inside the core, the field is concentrated within one elementary junction. The in-plane size of the DL core is much bigger, about 50 nm. That means that for a junction of $1 \mu\text{m}$, about 10 DLs can completely overlap its area and the voltage then drops on one elementary junction, as was observed experimentally.

Another consequence of that model is the prediction of a multiple periodic structure above the threshold voltage associated with the appearance of the first, second, and so on, DLs. That structure was experimentally found [32] (figure 7).

Note, here, the remarkable similarity between layered superconducting and CDW systems that manifests itself in similar mechanisms of phase decoupling via formation of phase vortices. In both cases a threshold energy for phase decoupling associated with H_{c1} or V_t is much less than the value of the energy gap. We summarize those features in table 1.

From the model it follows also that at $V \gg V_t$, when the DLs overlap, the phase difference in the weak junction grows

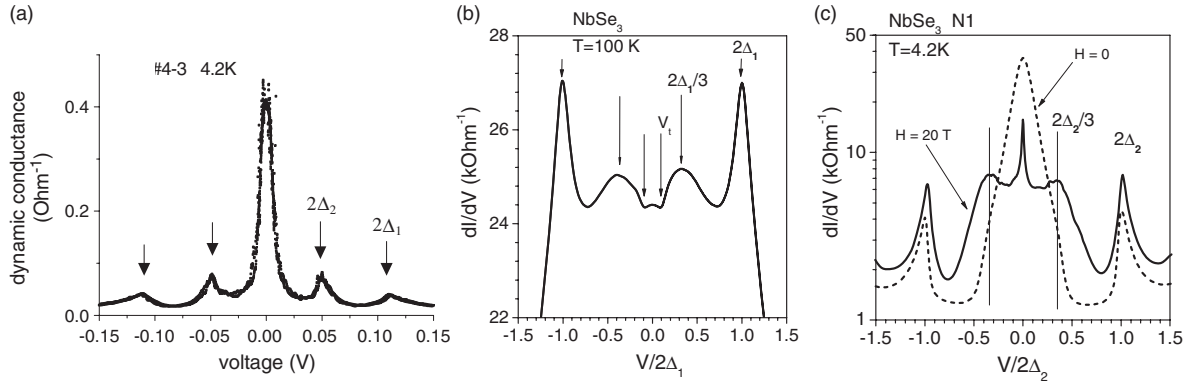


Figure 5. Interlayer tunnelling spectra of NbSe₃ at low temperature (a), high temperature (b) and at low temperature in the presence of a high magnetic field oriented parallel to the layers, $H \parallel c$ (c).

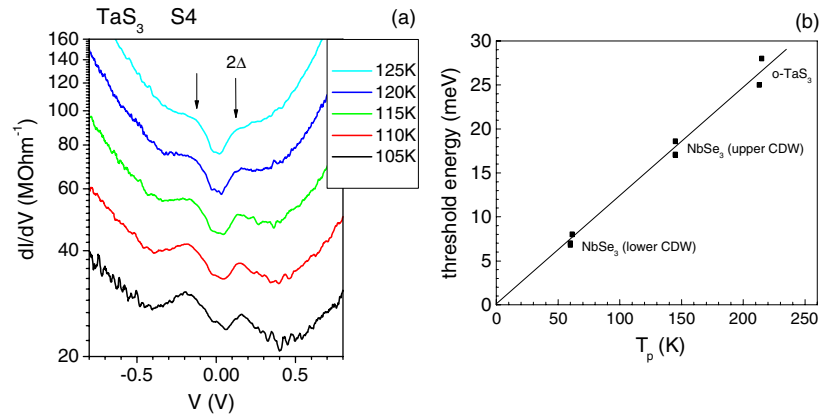


Figure 6. (a) Interlayer tunnelling spectra of o-TaS₃; (b) dependence of the threshold energy for interlayer tunnelling eV_t as a function of the Peierls transition temperature T_p . The straight line corresponds to the scaling relation $eV_t = 1.3kT_p$.

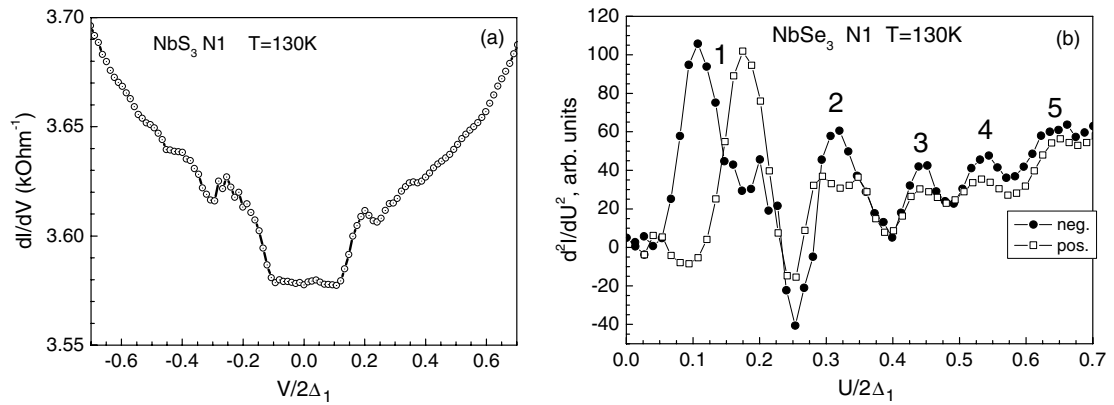


Figure 7. Threshold for interlayer tunnelling conductivity in a NbSe₃ stacked junction (a) and its staircase structure resolved on the second derivative picture (b).

linearly with a distance along the junction as

$$\varphi_1 - \varphi_2 = \frac{2Vx}{\hbar v_F}, \quad (3)$$

in a very similar way as the phase difference evolves in time in a Josephson junction at high bias voltage:

$$\varphi_1 - \varphi_2 = \frac{2Vt}{\hbar}. \quad (4)$$

8. Summary

The method of interlayer tunnelling spectroscopy has been adapted for studies of layered CDW materials of MX₃ type. Using this technique we identified CDW energy gaps and zero bias conductance peak and we found an interaction between two CDWs in NbSe₃ in the temperature range of their coexistence. We also found intragap states with an energy of

$2\Delta/3$ and $\approx 0.1\Delta$ that have been attributed to the amplitude and phase excitations of CDW.

Acknowledgments

The studies were supported by the Russian Fund of Basic Research, grant 05-02-17578-a, and by the Program of Presidium RAS ‘Quantum nanostructures’. The work was partially performed in the frame of CNRS-RAS Associated European Laboratory between CRTBT and IREE ‘Physical properties of coherent electronic states in condensed matter’.

References

- [1] Kleiner R, Steinmeyer F, Kunkel G and Mueller P 1992 *Phys. Rev. Lett.* **68** 2394
As a recent review, see Yurgens A 2000 *Supercond. Sci. Technol.* **13** R85
- [2] Tanabe K, Yidaka Y, Karimoto S and Suzuki M 1996 *Phys. Rev. B* **53** 9348
- [3] Krasnov V M, Yurgens A, Winkler D, Delsing P and Claeson T 2000 *Phys. Rev. Lett.* **84** 5860
- [4] Latyshev Yu I, Koshelev A E and Bulaevskii L N 2003 *Phys. Rev. B* **68** 134504
- [5] Latyshev Yu I, Kim S-J, Pavlenko V N, Yamashita T and Bulaevskii L N 2001 *Physica C* **362** 156
- [6] Bulaevskii L N, Clem J R and Glazman L I 1992 *Phys. Rev. B* **46** 350
- [7] Clem J R and Coffey M W 1989 *Phys. Rev. B* **42** 6209
- [8] Bulaevskii L N and Clem J R 1991 *Phys. Rev. B* **44** 10234
- [9] Latyshev Yu I, Gaifullin M B, Yamashita T, Machida M and Matsuda M 2001 *Phys. Rev. Lett.* **87** 247067
- [10] Nachtrab P, Helm S, Moessle M, Kleiner R, Waldmann O, Koch R, Mueller P, Kimura T and Tokura Y 2002 *Phys. Rev. B* **65** 012410
- [11] Latyshev Yu I, Monceau P, Sinchenko A A, Bulaevskii L N, Brazovskii S A, Kawae T and Yamashita T 2003 *J. Phys. A: Math. Gen.* **36** 9323
- [12] For details of the CDW ground state see Gruener G 1994 *Density Waves in Solids* (Reading, MA: Addison-Wesley)
- [13] Latyshev Yu I, Bulaevskii L N, Sinchenko A A, Pavlenko V N and Monceau P 2002 *JETP Lett.* **75** 93
- [14] Latyshev Yu I, Yamashita T, Bulaevskii N B, Graf M J, Balatsky A V and Maley M P 1999 *Phys. Rev. Lett.* **82** 5345
- [15] Krasnov V M, Santberg M and Zogai I 2005 *Phys. Rev. Lett.* **94** 077003
- [16] Latyshev Yu I, Kim S-J and Yamashita T 1999 *IEEE Trans. Appl. Supercond.* **9** 4312
- [17] Dai Z, Slough C G and Coleman R V 1991 *Phys. Rev. Lett.* **66** 1318
- [18] Perucci A, Degiorgi L and Thorne R E 2004 *Phys. Rev. B* **69** 195114
- [19] Schaefer J, Sing M, Claessen R, Rotenberg E, Zhou X J, Thorne R E and Kevan S D 2003 *Phys. Rev. Lett.* **91** 066401
- [20] Bae M-H, Choi J-H, Lee H-J and Park K-S 2005 Interplay between superconducting and pseudogap states revealed by heating compensated interlayer tunnelling spectroscopy on $\text{Bi}_2\text{Sr}_2\text{CaCu}_2\text{O}_{8+x}$ *Preprint cond-mat/0512664*
- [21] Orlov A P, Latyshev Yu I, Smolovich A M and Monceau P 2006 *JETP Lett.* **84** 89
- [22] Moudren A H, Axe J D, Monceau P and Levy F 1990 *Phys. Rev. Lett.* **65** 223
- [23] Fleming R M, Moncton D E and McWan D B 1978 *Phys. Rev. B* **18** 5560
- [24] Ayari A, Danneau R, Reguardt H, Ortega L, Lorenzo J E, Monceau P, Currat R, Brazovskii S and Grubel G 2004 *Phys. Rev. Lett.* **93** 106404
- [25] Lee P A and Rice T M 1979 *Phys. Rev. B* **19** 3970
- [26] Bruinsma R and Trullinger S E 1980 *Phys. Rev. B* **22** 4543
- [27] Richard J and Monceau P 1980 *Solid State Commun.* **33** 635
- [28] Brazovskii S A 1980 *Sov. Phys.—JETP* **51** 342
- [29] Latyshev Yu I, Monceau P, Brazovskii S, Orlov A P and Fournier T 2005 *Phys. Rev. Lett.* **95** 266402
- [30] Latyshev Yu I, Monceau P, Brazovskii S A, Orlov A P, Sinchenko A A, Fournier Th and Mossang E 2005 *J. Physique IV* **131** 197
- [31] Brazovskii S, Latyshev Yu I, Matveenko S I and Monceau P 2005 *J. Physique IV* **131** 77
- [32] Latyshev Yu I, Monceau P, Brazovskii S, Orlov A P and Fournier T 2006 *Phys. Rev. Lett.* **96** 116402